Half the world's population already experiences a climate 1.5°C warmer than preindustrial

Chris Brierley[a,*], Alexander Koch[a], Maryam Ilyas[b,c], and Natalie Wennyk[a]

[a]Department of Geography, University College London, London, U.K.
[b]Department of Statistical Science, University College London, London, U.K.
[c]College of Statistical and Actuarial Sciences, University of the Punjab Lahore, Pakistan
[*]c.brierley@ucl.ac.uk

The world has warmed appreciably over the past two centuries (Fig. 1a). The Paris Agreement commits the world to keeping global mean temperature 'well-below 2 °C' above preindustrial[1]. This value is a global average and some regions will experience warming much greater than this, for example the Arctic[2]. Such a regional pattern can make it hard for people to associate the global threshold with their local experiences[3]. The long timescales of climate change provide a further challenge: not only does interannual variability obscure the multi-year average, but the preindustrial reference state was multiple generations ago[4].

The Paris Agreement does not provide a precise definition of when the preindustrial reference period occurred[1]. For practical reasons, it is often taken as the average of 1850–1900 CE[5,6], because this is earliest that we have sufficient global coverage of instrumental records. An earlier reference period would be desirable from a radiative forcing perspective[7], because humans had already noticeably altered the climate system by the early instrumental period[8,9]. An expert assessment states that the earlier reference period was cooler than the 1850–1900 CE instrumental period[6,7], with a subsequent model-based quantification finding it up to 0.1 °C cooler[10]. The uncertainty in the amount of warming that has already occurred also differs between the instrumental and earlier baselines[10]. The uncertainty in the preindustrial baseline temperature even propagates into the estimate of well-observed years[7] (Fig. 1b). There is ongoing discussion about the most appropriate definition of the preindustrial baseline[11,12]. Here we apply the stricter definition of a long-term average climate prior to industrialisation[10] (taken as 1400–1800 CE, Methods), rather than assume the early instrumental period[5,6] (1850–1900 CE) represents "preindustrial" conditions.

Regional temperature changes are rarely presented with respect to the preindustrial. For example, they were never shown this way in the IPCC's 5th Assessment Report[5], upon which the Paris Agreement was grounded. The recent IPCC special report[6] "Global Warming of 1.5 °C" was the first to show temperature plots with respect to a preindustrial baseline. Choosing not to present changes from preindustrial may be justified given the uncertainty in our knowledge of the preindustrial baseline (for example Fig. 1b implies less confidence in warming trend than Fig. 1a). However, it can mislead observers about the magnitude of warming that has occurred. Here we provide and display an ensemble of gridded temperature observations that shows the warming since preindustrial and its uncertainty.

The sparse instrumental coverage prior to the 1950s means that even the state of the El Niño-Southern Oscillation may be ambiguous[13], despite being the dominant mode of climate variability[14]. This means that when calculating regional temperature changes from any preindustrial baseline one must also formally quantify the uncertainties, especially those associated with the regions without instrumental coverage[15]. Here we base our dataset on the HadCRUT4 compilation of station observations[16] combined with multi-resolution lattice kriging[15] to retain covariance relationships at global, synoptic and local scales. 10,000 equally-plausible ensemble members represent the observed temperature change, beginning in 1850 CE[13] (Methods).

Reconstructing the spatial pattern of the warming prior to reliable instrumental coverage (pre-1850 CE) presents a different challenge. The forced component of global warming of the early instrumental period (1850–1900 CE) with respect to 1400–1800 CE has been estimated from a 26-member multi-model ensemble of climate simulations covering the past millennium[10]. The global mean warming is often used as an index of climate change, because local changes and many impacts scale approximately linearly with it[1]. Unfortunately conventional pattern-scaling tools are not appropriate to expand the global mean offsets spatially, because they either cannot represent cold states prior to the future projections[17] or realistic covariance sampling[18].

Here we adopt a novel pattern-scaling approach that not only reconstructs the mean pattern and local uncertainty, but critically also retains the spatial covariances between locations in its reconstructed patterns (Methods). In brief, an ensemble of scalable patterns were created from the regression slopes of the first 10 empirical orthogonal functions of the merged surface temperatures changes seen in CMIP5 under the RCP2.6 scenario, combined with a residual term. We multiply these scalable patterns by the global mean warming from the preindustrial to the early instrumental[10] and combine with the spatially-complete temperature observations[13] to create an annual-resolution dataset of local temperature anomalies from the preindustrial along with quantified uncertainties. The median difference in temperature of the preindustrial from the projection reference period of

AR5[5] (1986–2015 CE) is statistically significant across the most of the globe (Fig. 2a).

2016 CE was globally the warmest year on record (Fig. 2b, at the time of writing) through the combination of anthropogenic forcing and a very strong El Niño[14]. There is a very small probability (3.6%) that the global mean temperature in 2016 CE was 1.5 °C or more above the preindustrial. We stress that the reason this probability exists is becuase of uncertainty related to the preindustrial reference period, rather than the quality of the temperature observations in 2016 CE (c.f. Fig. 1a,b). The proportion of the globe in 2016 CE with an annual temperature anomaly greater than 1.5 °C was 31.1% (IQR of 27.5-34.9%); and 16.2% (14.1-18.6%) saw temperatures over 2 °C (Fig. 3a, Tab. **??**).

As well as temperatures rising since the preindustrial, the global population has increased dramatically[19] (Fig. 3b). People are not evenly spread across the globe: the vast majority live on the land, which warms faster the ocean[20]. Assessing the direct health impacts of the warming requires consideration of only the temperatures to which people are exposed - rather than the global average[21]. The majority of the world's population lives in Asia[19], yet very few live in the portion of it that saw the warmest temperature anomalies in 2016 CE (Siberia was more than 2.5 °C above preindustrial; Fig. 2b).

A further major demographic trend over the past two centuries has been the shift to living in towns and cities instead of the countryside[19]. Due to the urban heat island effect[22], this shift itself will lead to people on average being exposed to higher temperatures. Whilst estimates of the urban heat island effect exist with global coverage[23], information about of their evolution since 1850 CE does not. We therefore incorporate the impact of urbanisation as a time invariant adjustment felt by an increasing proportion of the population (Methods).

Combining the temperature dataset with both population information and the urbanisation adjustments allows the number of people living at various warming levels to be determined each year (Fig. 3a; Fig. 4). The total number of people that experience an annual mean temperature at, or below, the preindustrial level in each year has not increased, despite the substantial population growth (Fig. 3a). Whilst as percentage, it has dropped throughout the industrial era and is effectively negligible now (Fig. 4). It is as if all the population growth since industrialisation has occurred at elevated temperatures.

The Lancet Countdown[21] defines one indicator for the health effects of temperature change as the 'exposure-weighted' average temperature (i.e. the temperature change experienced by a person on average). The report stressed that this indicator increased at double the rate of global (area-weighted) temperature since 2000 CE[21]. The temperature anomaly dataset and urban heat island methodology developed here means it is possible to 'exposure-weight' the warming since the preindustrial for the first time. This indicator consistently shows larger changes with respect to the preindustrial (Fig. 1c) than the global mean temperature since 1850 CE (Fig. 1b). It is possible to explore the reasons for this difference (Fig. **??**). Firstly, the human population is not distributed evenly over the globe[19], increasing the global average by 0.2 °C. Secondly, urbanisation exposes people to warmer temperatures[22], which has a noticeable effect on the global average experienced. The effect of both demographic trends is visible throughout the instrumental record[21] (Fig. **??**).

The impact of considering the relative population sizes when thinking about observed temperature changes across the globe are best illustrated through the use of cartograms[24]. Fig. 5 presents the national average warming since the preindustrial for 2016 CE: using (a) area weighting and (b) both exposure-weighting and scaling each country's size relative to its national population. The differing impacts of considering the exposure-weighted and area-weighted averages is most noticeable in North America. The U.S. population has experienced a greater warming than its area average, in part due to its high urban population. Meanwhile Canadians predominantly do not live within the Arctic Circle and so are not exposed to the extreme warming happening there.

Natural year-to-year variations can mean there are always regions of the globe that experience temperature at or below the preindustrial, as well as substantially warmer than that (Fig. 2) Nonetheless as the global population crossed 2 billions in the 1930s, it also crossed into a world where, for the first time, less people were exposed to a preindustrial climate than a world with warming of 1 °C or higher (Fig. 4). Our analysis shows that 1990 CE was the first year that 50% of the world's population was exposed to 1 °C above preindustrial. Since the Kyoto Protocol was signed in 1997 CE, a majority of the world's population has lived in temperatures 1 °C or more above preindustrial (Fig. 4). We find that in 2015 CE over half of the global population was exposed to temperature greater than 1.5 °C above preindustrial (55%, Tab. **??**).

The Paris Agreement[1] commits us to "pursuing efforts to limit [global average] temperature increase to 1.5 °C". The ensemble of patterns used to create the preindustrial baseline can also be scaled to represent the regional temperatures associated with various global mean temperatures. This allows estimation of the amount of people that experienced local temperatures equivalent to a global mean temperature rise of 1.5 °C or more each year (Fig. **??**). By the time of the Rio Earth Summit in 1992 CE, the proportion of the global population experiencing preindustrial conditions was smaller than that experiencing global temperatures above the 1.5 °C goal of the Paris Agreement (Fig. **??**). We estimate that in 2015 CE half of world's population experienced annual mean temperatures equivalent to a global warming of 1.5 °C above preindustrial - a third of whom only did so because of urban heat island effects (Tab. **??**).

The Paris Agreement is highly, yet necessarily, ambitious in its desire to limit temperature to 1.5 °C above preindustrial[1]. While the reference to a preindustrial baseline is justifiable, it introduces additional uncertainty into the observed temperature increases[7,11,12]. Having devised a methodology to account for the local expression of this uncertainty, we explore the spatial pattern of temperature changes from both geographic and demographic perspectives. Most people alive today are unlikely to have ever experienced preindustrial temperatures, especially given an increasing urban population exposed to urban heat island effects. Indeed the majority of the world's population has already experienced annual temperatures above 1.5 °C, and the remainder is likely to experience temperatures equivalent to a 1.5 °C world much earlier than the planet itself. Given the global population's current exposure to warmer temperatures, it is clear that we should stop thinking of climate change primarily in the future tense.

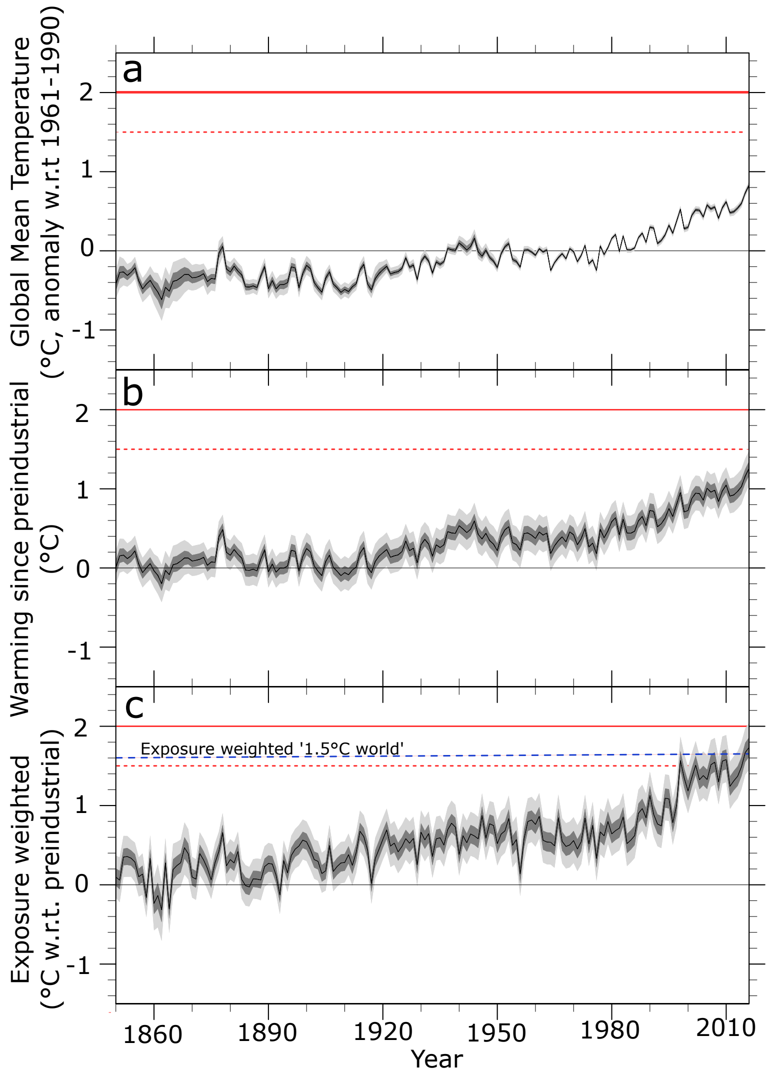

Figure 1. Global mean, annual average temperature change. The median, interquartile and 5–95% ranges[13] with respect to (a) the 1961–1990 CE climatological period and (b) the preindustrial. (c) The average global temperature weighted by exposure[21] (i.e. population including an urban heat island adjustment). The median, interquartile and 5–95% ranges are shown with respect to the preindustrial [note that the uncertainty range in (c) does not include uncertainty in the population distribution or urban heat island, which are not fully-quantified in the underlying datasets]. The dashed blue line shows the (median) equivalent of a 1.5 °C warmer world derived from the pattern-scaling (see Methods).

References

1. United Nations Framework Convention on Climate Change. *Adoption of the Paris Agreement FCCC/CP/2015/10/Add.1* (2015).

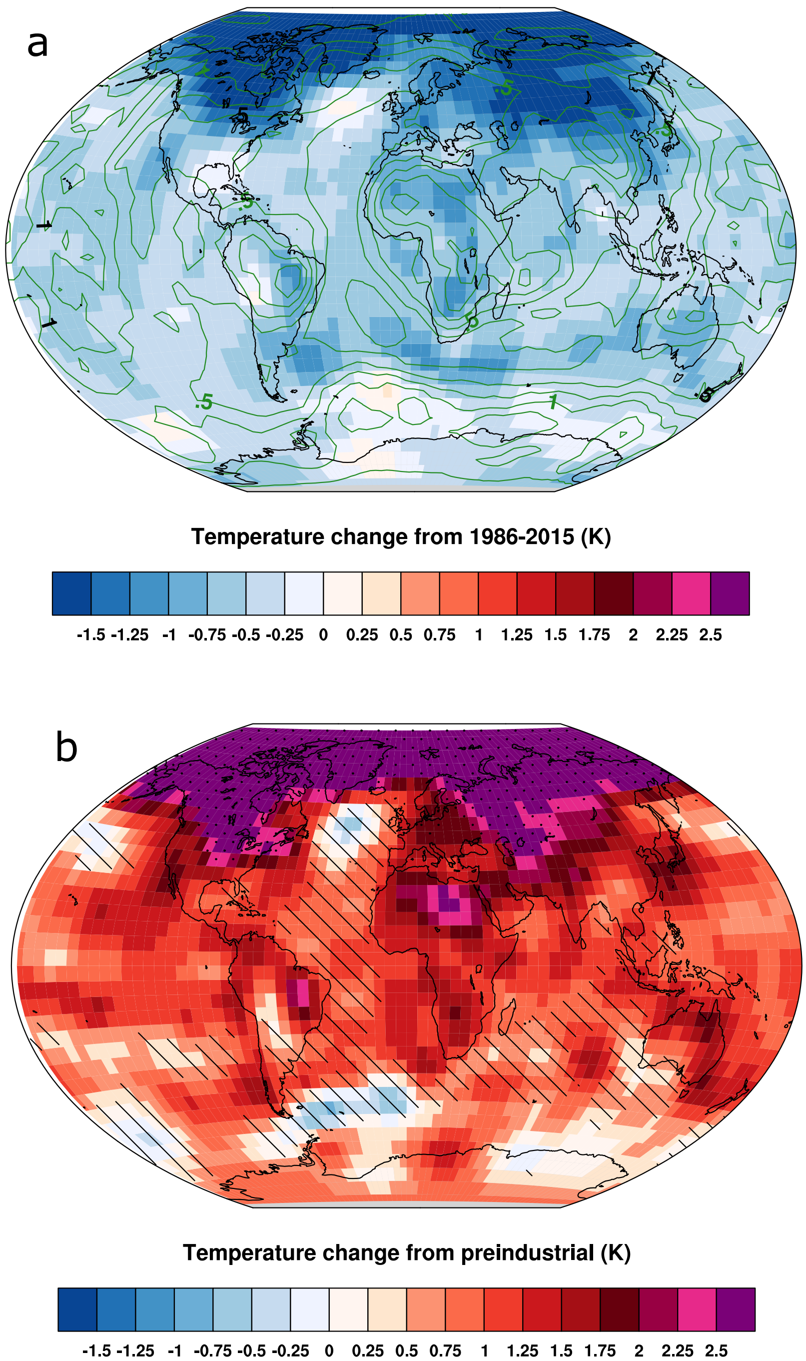

Figure 2. Spatial patterns of temperature change. (a) The median annual average offset of the preindustrial period from the 1961–1990 CE climatology, along with the interquartile range (green contours) in the offset. (b) The annual temperature of 2016 CE above preindustrial. Cross-hatching indicates regions that are not significantly different from the preindustrial at the 5% confidence level. Stippling shows regions that are at 1.5 °C or higher at the 5% confidence level.

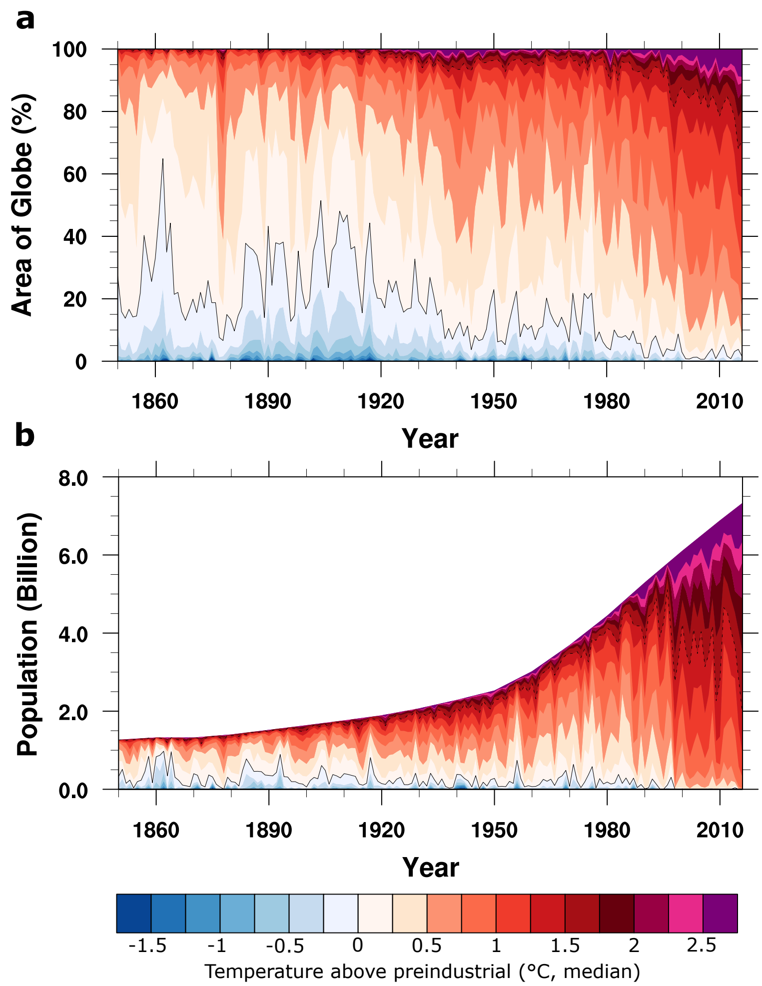

Figure 3. Subdividing global area and population by warming. (a) The proportion of the global area at particular (median) annual temperatures in each year. (b) The population[19] exposed to particular (median) annual temperatures in each year since 1850 CE. The preindustrial and +1.5 °C are indicated by black solid and dashed lines respectively.

2. Serreze, M. C. & Barry, R. G. Processes and impacts of arctic amplification: A research synthesis. *Glob. planetary change* **77**, 85–96 (2011).

3. Howe, P. D., Markowitz, E. M., Lee, T. M., Ko, C.-Y. & Leiserowitz, A. Global perceptions of local temperature change. *Nat. Clim. Chang.* **3**, 352 (2013).

4. Hulme, M., Dessai, S., Lorenzoni, I. & Nelson, D. R. Unstable climates: Exploring the statistical and social constructions of 'normal'climate. *Geoforum* **40**, 197–206 (2009).

5. Hartmann, D. L. *et al.* Observations: atmosphere and surface. In *Climate Change 2013 the Physical Science Basis: Working Group I Contribution to the Fifth Assessment Report of the Intergovernmental Panel on Climate Change* (Cambridge University Press, 2013).

6. Allen, M. *et al.* Framing and context. In *Global Warming of 1.5°C: an IPCC special report* (Cambridge University Press, 2018).

7. Hawkins, E. *et al.* Estimating changes in global temperature since the pre-industrial period. *Bull. Am. Meteorol. Soc.* (2017).

8. Schurer, A. P., Hegerl, G. C., Mann, M. E., Tett, S. F. & Phipps, S. J. Separating forced from chaotic climate variability over the past millennium. *J. Clim.* **26**, 6954–6973 (2013).

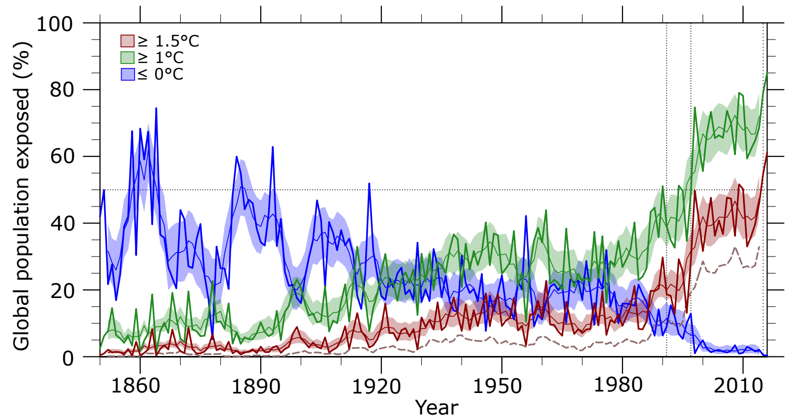

Figure 4. Exposure to annual mean temperatures. The proportion of the global population exposed to various temperature levels: at or below the preindustrial (blue); +1 °C above preindustrial (green); and +1.5 °C. The thick line shows the annual median value, whilst the thin lines show the 5-year running median temperature estimates along with its interquartile range. The dashed pink line shows the +1.5 °C exposure, without considering the urban heat island. Dotted vertical lines indicate major international commitments to tackle climate change in 1992 CE (Rio), 1997 CE (Kyoto) and 2015 CE (Paris).

9. Koch, A., Brierley, C., Maslin, M. M. & Lewis, S. L. Earth system impacts of the European arrival and Great Dying in the Americas after 1492. *Quat. Sci. Rev.* **207**, 13–36 (2019).

10. Schurer, A. P., Mann, M. E., Hawkins, E., Tett, S. F. & Hegerl, G. C. Importance of the pre-industrial baseline for likelihood of exceeding Paris goals. *Nat. Clim. Chang.* **7**, 563–567 (2017).

11. Schurer, A. *et al.* Interpretations of the Paris climate target. *Nat. Geosci.* **11**, 220 (2018).

12. Millar, R. J. *et al.* Reply to 'Interpretations of the Paris climate target'. *Nat. Geosci.* **11**, 222–222 (2018).

13. Ilyas, M., Brierley, C. M. & Guillas, S. Uncertainty in regional temperatures inferred from sparse global observations: Application to a probabilistic classification of El Niño. *Geophys. Res. Lett.* **44**, 9068–9074 (2017). DOI 10.1002/2017GL074596. 2017GL074596.

14. Huang, B., L'Heureux, M., Hu, Z.-Z. & Zhang, H.-M. Ranking the strongest ENSO events while incorporating SST uncertainty. *Geophys. Res. Lett.* **43**, 9165–9172 (2016).

15. Nychka, D., Bandyopadhyay, S., Hammerling, D., Lindgren, F. & Sain, S. A multi-resolution Gaussian process model for the analysis of large spatial data sets. *J. Comput. Graph. Stat.* **24**, 579–599 (2015).

16. Morice, C. P., Kennedy, J. J., Rayner, N. A. & Jones, P. D. Quantifying uncertainties in global and regional temperature change using an ensemble of observational estimates: The HadCRUT4 data set. *J. Geophys. Res. Atmospheres* **117**, n/a–n/a (2012). DOI 10.1029/2011JD017187. D08101.

17. Tebaldi, C. & Arblaster, J. M. Pattern scaling: Its strengths and limitations, and an update on the latest model simulations. *Clim. Chang.* **122**, 459–471 (2014).

18. Osborn, T. J., Wallace, C. J., Harris, I. C. & Melvin, T. M. Pattern scaling using climgen: monthly-resolution future climate scenarios including changes in the variability of precipitation. *Clim. Chang.* **134**, 353–369 (2016).

19. Goldewijk, K. K., Beusen, A., Doelman, J. & Stehfest, E. Anthropogenic land use estimates for the Holocene–HYDE 3.2. *Earth Syst. Sci. Data* **9**, 927–953 (2017).

20. Joshi, M. M., Gregory, J. M., Webb, M. J., Sexton, D. M. & Johns, T. C. Mechanisms for the land/sea warming contrast exhibited by simulations of climate change. *Clim. Dyn.* **30**, 455–465 (2008).

21. Watts, N. *et al.* The Lancet Countdown on health and climate change: from 25 years of inaction to a global transformation for public health. *The Lancet* **391**, 581–630 (2018).

22. Oke, T. R. The energetic basis of the urban heat island. *Q. J. Royal Meteorol. Soc.* **108**, 1–24 (1982).

23. Center for International Earth Science Information Network, Columbia University. Global urban heat island (UHI) data set, 2013 (2016). DOI 10.7927/H4H70CRF.

24. Dorling, D., Barford, A. & Newman, M. Worldmapper: the world as you've never seen it before. *IEEE Trans. Vis. Comput. Graph.* **12**, 757–764 (2006).

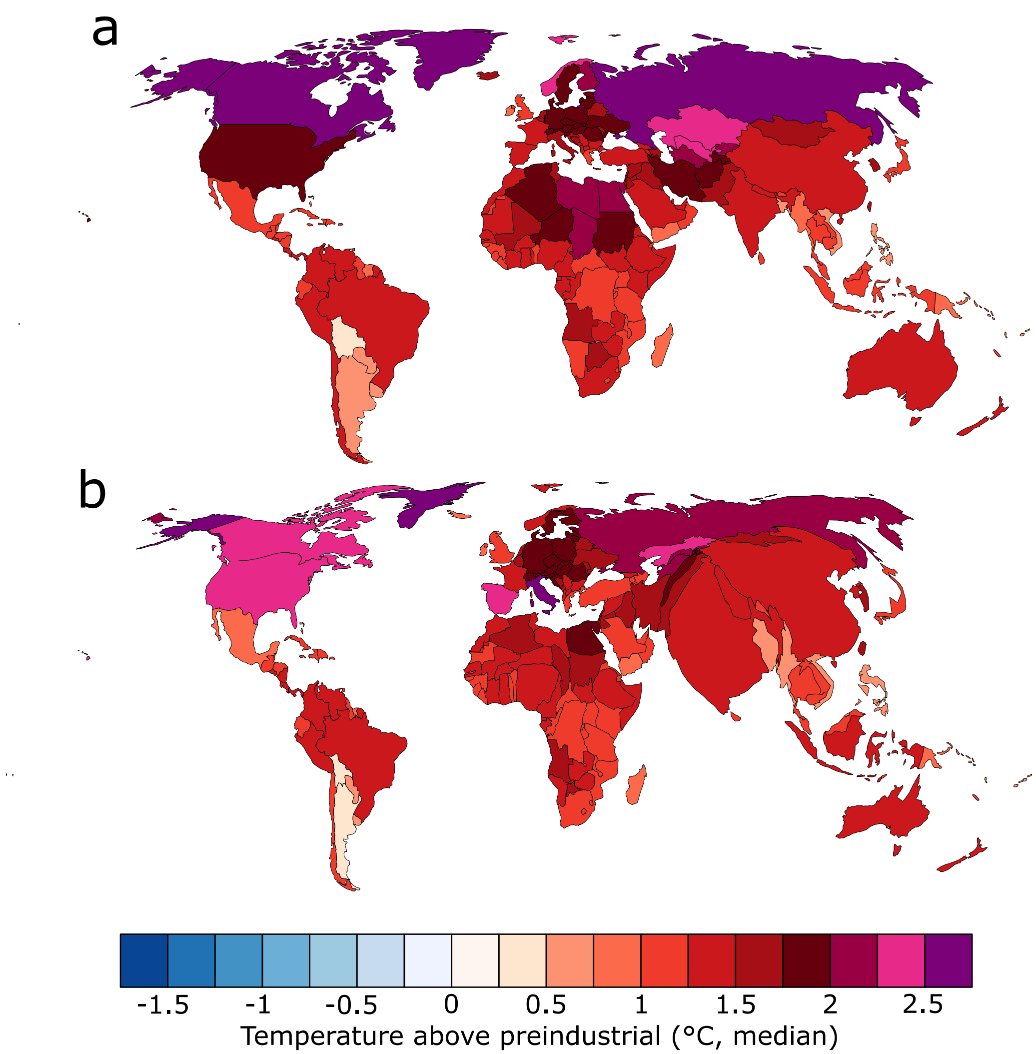

Figure 5. Two representations of the 2016 annual temperature anomalies at a national level. (a) A conventional cartogram, where a nation is coloured according to its area-averaged temperature anomalies. (b) An exposure-weighted cartogram, where a country's size is determined by its population, and the colour is the exposure-weighted temperature anomaly, incorporating the urban heat island[24]. Note: Alaska is treated as an independent nation for the purposes of these representations.